

## MISORIENTATION BETWEEN AUSTENITE AND $\sigma$ -PHASE IN DUPLEX STAINLESS STEEL

Tibor BEREZC and Péter J. SZABÓ

Department of Materials Science and Engineering  
Budapest University of Technology and Economics  
H–1111 Budapest, Goldmann tér 3. V2/153.  
e-mails: berezc.tibor@freemail.hu, szpj@eik.bme.hu

Received: March 8, 2005

### Abstract

Duplex steels are very interesting stainless steels. Their name originates from their special austenitic-ferritic structure. This tissue is due to the high alloying and low carbon content. During heat treatment, several phase transformation and precipitation processes take place.

Electron back scattering diffraction is a relatively new investigation method, by which the individual grain orientation can be determined in the scanning electron microscope. The greatest advantage of this method is its speed: it is possible to determine a grain orientation even within 0.1 second. Therefore, in a relatively short time a large amount of data can be collected, and can be statistically evaluated.

This paper reports a research work, in which SAF-2507 type duplex stainless steel samples were heat-treated isothermally, and the misorientation between the austenite and  $\sigma$ -phase was calculated.

*Keywords:* duplex stainless steel,  $\sigma$ -phase, austenite, EBSD, misorientation.

### 1. Introduction

Duplex steels are high alloyed corrosion resistant steels. Their microstructure mainly consists of austenite ( $\gamma$ ) and ferrite ( $\alpha$ ). Ferrite improves corrosion resistance against stress-, pitting- and crevice-corrosion, while austenite ensures the formability, toughness and weldability [1]. The required ferrite/austenite ratio can easily be adjusted by up-to-date metallurgical technologies.

Nowadays the application of duplex steels has increased in some special cases as well. Seawater environment requires the special properties of duplex steels: bridges, oil towers, tankers are made of this material.

Generally speaking, it is valid for these steels that as the amount of alloying elements increases, the probability of precipitation processes is larger. Therefore, it is necessary to keep the carbon content as low as possible. Chromium alloying increases the corrosion resistance, nickel alloying increases toughness. The effect of nitrogen is to increase the resistance against pitting corrosion and to improve strength. These three alloying elements can be found in all duplex steels.

Very often these steels are alloyed with molybdenum, but alloying with tungsten and copper depends on regional and metallurgical aspects. Due to W and Mo additives, the steel withstands local corrosion. Tungsten helps to build a compact

WO<sub>3</sub> layer on the surface. Some authors report experiments in which a part of the tungsten is substituted by molybdenum, some investigated the effect of tungsten on the stability of  $\delta/\gamma$  phases, and on the kinetics of other intermetallic precipitation [8, 9].

Due to the high alloying content, several intermetallic precipitations, as well as phase transformations occur during heat treatment or welding. The most important intermetallics are the  $\sigma$ ,  $\chi$ , Cr<sub>2</sub>N, M<sub>23</sub>C<sub>6</sub> and  $\alpha'$  phases (the latter is responsible for the embrittlement at 475 °C). Precipitation of these phases occurs mostly in the vicinity of ferrite, since diffusion processes are faster in ferrite than in austenite [6]. These precipitation processes take place between 400 and 600 °C.

Between 600 and 900 °C the ferrite (after a certain incubation time) starts to decompose into secondary austenite and  $\sigma$ -phase ( $\alpha \rightarrow \gamma_2 + \sigma$ ) [10]. Occurrence of  $\sigma$ -phase is the most likely at ferrite/austenite boundaries where the misorientation deviates the most from the KURDJUMOV–SACHS relationship [12], which has the lowest boundary energy [13]. The formation of  $\sigma$ -phase at the ferrite/austenite boundary is preceded by M<sub>23</sub>C<sub>6</sub> carbide precipitation [14].

In order to investigate the precipitation mechanism, it is necessary to determine the orientation relationship between the matrix and the precipitated material. NENNO et al. [11] suggested the following relationship in 1962, according to pure crystallographic calculations:

$$(111)_\gamma \parallel (001)_\sigma \quad \text{and} \quad [\bar{1}01]_\gamma \parallel [110]_\sigma$$

or, what is very similar:

$$(111)_\gamma \parallel (001)_\sigma \quad \text{and} \quad [0\bar{1}\bar{1}]_\gamma \parallel [140]_\sigma.$$

The difference between the above two orientation relationships is less than one degree. According to their calculation, these two connections mean the lowest interfacial energy between the austenite and  $\sigma$ -phase.

However, practical heat treatments rarely help to form the optimal orientation relationship. According to CHEN and YANG [4], annealing between 1020 and 1080 °C and subsequent slow cooling (0.1 °C/s) cause the misorientation between austenite and  $\sigma$ -phase to differ from Nenno-relationship. This difference can even be 10–12 degrees.

## 2. Sample Preparation

The nominal chemical composition of duplex steel can be seen in *Table 1*.

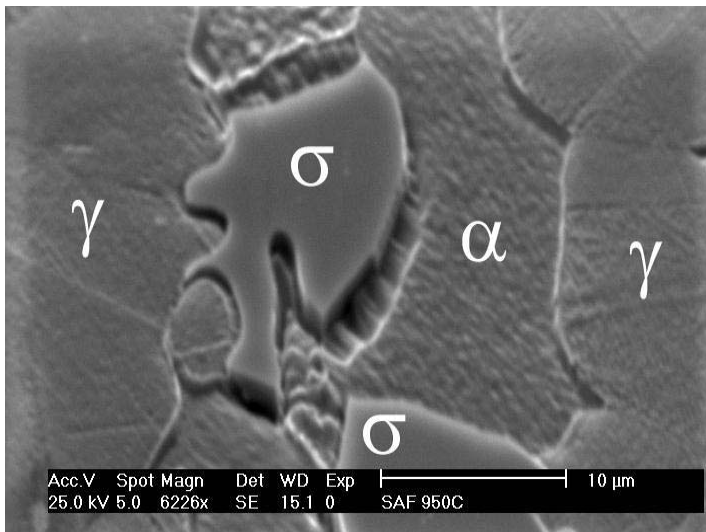
This work focuses on how the change of the parameters of the heat treatment affects the orientation relationship between the austenite and the  $\sigma$ -phase. Therefore, samples were heat treated at 900 °C for 100, 200, 500 and 1000 s. After this, samples were ground and polished by traditional metallographic methods. A special final polishment was done for EBSD-measurements by fine grain colloid silica (grain size was 0.02  $\mu\text{m}$ ) for at least 20 min in order to remove the Beilby-layer.

Table 1. Chemical composition of duplex steel

C [wt %]	Cr [wt %]	Ni [wt %]	Mo [wt %]	W [wt %]	Cu [wt %]	N [wt %]	Fe
max. 0.03	22–25	4–7	0–4	0–2	0–1.5	0.1–0.35	bal.

### 3. Experimental Method

The samples were investigated by electron back scattering diffraction (EBSD). *Fig. 1* shows a typical structure of the material (secondary electron image, taken in the scanning electron microscope). Austenite ( $\gamma$ ), ferrite ( $\alpha$ ) and  $\sigma$ -phase are indicated in the figure.



*Fig. 1.* Typical structure of the SAF 2507 type duplex steel. Austenite ( $\gamma$ ), ferrite ( $\alpha$ ) and  $\sigma$ -phase are indicated. Secondary electron image.

The orientation relationship between the austenite and the  $\sigma$ -phase was determined by electron back scattering diffraction (EBSD). In this method, an electron beam in the scanning electron microscope penetrates the surface of the sample, which is tilted at an angle of 70 degrees. In the top layer of the sample the incident electrons are inelastically scattered, and then forward diffracted elastically according to Bragg's Law. Diffracted electrons leave the crystal along two cones (*Fig. 2*). On a suitably positioned fluorescent screen the interception of the cones and the plane of the screen appear. These are the so-called *Kikuchi-lines*.

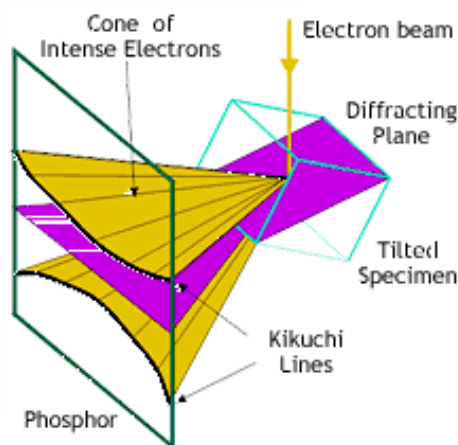


Fig. 2. Formation of Kikuchi-lines

By adequate software, the crystallographic orientation of the excited point can be determined. A great advantage of the EBSD-technique is its speed: it is possible to evaluate even more than 10 points within a second. This allows the user to make orientation maps, since creating a map containing 30 000 points takes less than an hour. Such an orientation map is shown in Fig. 3, where the individual orientations of the measured points are given by the colour coding (or grayscale coding) of the basic triangle of the inverse pole figure.

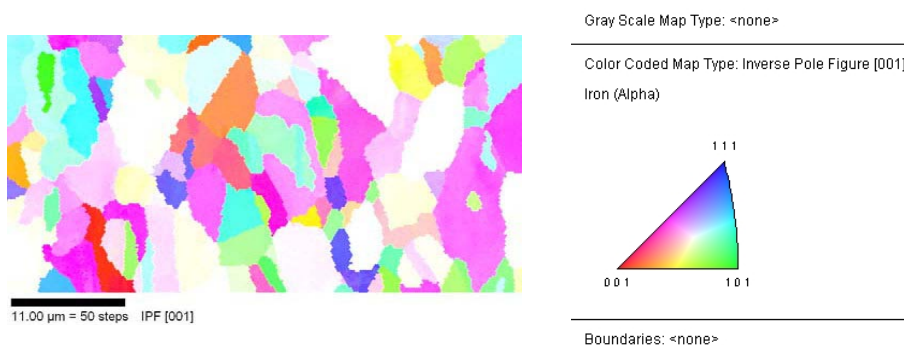


Fig. 3. Inverse pole figure map. The individual orientations of the different measuring points are given by the colour coding of the base triangle of the inverse pole figure.

Further information about the EBSD-technique can be found elsewhere [2, 3]. In case of the present investigations, a Philips XL-30 scanning electron microscope and a TSL-EDAX EBSD-system were used.

#### 4. Results

The orientation relationship between austenite and  $\sigma$ -phase was determined by EBSD. At least five phase boundaries were measured in each sample, and the misorientation was determined by averaging at least ten measuring points at every phase boundaries. According to the literature, the best orientation fit is given by the Nenno orientation relationship [4].

The face centred cubic (FCC) austenite has 24 symmetry operators, the tetragonal  $\sigma$ -phase has 8 symmetry operators [5, 7]. This means that the general Nenno-relationship can be realized in  $24 \times 8 = 192$  ways.

Since the results of orientation determination by EBSD were in the form of matrices, it was necessary to determine the matrix formulation of the Nenno-relationship.

First, the difference between the two crystal structures should be taken into account by the deformation matrix, where the diagonal of the matrix shows the ratio of the lattice constants of the two structures [5]:

$$\mathbf{D} = \begin{bmatrix} \eta_1 & 0 & 0 \\ 0 & \eta_1 & 0 \\ 0 & 0 & \eta_2 \end{bmatrix} = \begin{bmatrix} \frac{a_\sigma}{a_\gamma} & 0 & 0 \\ 0 & \frac{b_\sigma}{b_\gamma} & 0 \\ 0 & 0 & \frac{c_\sigma}{c_\gamma} \end{bmatrix} \\ = \begin{bmatrix} 2.441667 & 0 & 0 \\ 0 & 2.441667 & 0 \\ 0 & 0 & 1.261111 \end{bmatrix}$$

Lattice constants are given in Table 2 [6].

Table 2. Lattice constant and lattice type of the measured  $\gamma$  and  $\sigma$  phase

Phase	Lattice constant (pm)			Lattice type
	a	b	c	
$\gamma$	360	360	360	FCC
$\sigma$	879	879	454	tetragonal

Nenno-relationship will be then given by the deformation matrix and the coordinate transformation matrix. The latter is determined by rotating two identical cubes into the Nenno-position by two rotations.

Let us first rotate the cube around face diagonal  $t$  by angle  $\omega_1$  (Fig. 4). The rotation angle can be calculated from the ratio of the edge and face diagonal of the cube:

$$\text{tg } \omega_1 = \frac{a\sqrt{2}}{a},$$

from which  $\omega_1 = 54.74^\circ$ .

Rotation angles of the rotation matrix can be calculated from the scalar products of axis  $t$  (as a vector, it is  $t_1 = [-110]$ ) and the three base vectors of the cube:  $\alpha_1 = 135^\circ$ ,  $\beta_1 = 45^\circ$ ,  $\gamma_1 = 90^\circ$ .

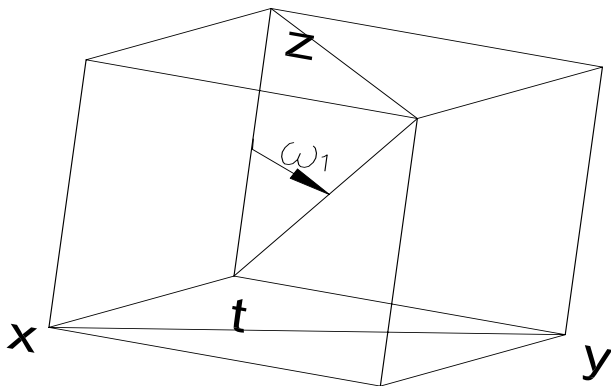


Fig. 4. Rotation around axis  $t$

Thus the matrix of this rotation is:

$$\mathbf{R}_1 = \begin{bmatrix} \frac{1}{2} \left(1 + \frac{1}{\sqrt{3}}\right) & -\frac{1}{2} \left(1 - \frac{1}{\sqrt{3}}\right) & \frac{1}{\sqrt{3}} \\ -\frac{1}{2} \left(1 - \frac{1}{\sqrt{3}}\right) & \frac{1}{2} \left(1 + \frac{1}{\sqrt{3}}\right) & \frac{1}{\sqrt{3}} \\ -\frac{1}{\sqrt{3}} & -\frac{1}{\sqrt{3}} & \frac{1}{\sqrt{3}} \end{bmatrix}$$

This matrix is orthonormal, since  $\det(\mathbf{R}_1) = 1$ . Note that in the case of face diagonal the body diagonal ratios are  $\sin(54.74^\circ) = \frac{\sqrt{2}}{\sqrt{3}}$  and  $\cos(54.74^\circ) = \frac{1}{\sqrt{3}}$ .

According to Fig. 5, it can be seen that the second rotation around the body diagonal has an angle of  $\omega_2 = 210$  degrees clockwise, because the shape of a cube viewing from the body diagonal direction is a hexagon, and the  $\bar{1}01$  direction is perpendicular to an edge of the hexagon. The  $[110]$  direction (face diagonal of the rotated cube) coincides with a diagonal of the hexagon. The axis of the rotation is the body diagonal, i.e. the vector  $t_2 = [111]$ . Angles of the rotation matrix are  $\alpha_2 = \beta_2 = \gamma_2 = 54.74^\circ$ .

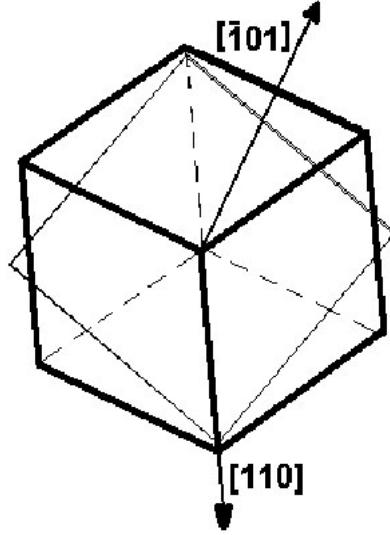


Fig. 5. Rotation around the body diagonal

Thus the matrix is:

$$\underline{\mathbf{R}}_2 = \begin{bmatrix} -\frac{1}{\sqrt{3}} \left(1 - \frac{1}{\sqrt{3}}\right) & \frac{1}{\sqrt{3}} \left(1 + \frac{1}{\sqrt{3}}\right) & \frac{1}{3} \\ \frac{1}{3} & -\frac{1}{\sqrt{3}} \left(1 - \frac{1}{\sqrt{3}}\right) & \frac{1}{\sqrt{3}} \left(1 + \frac{1}{\sqrt{3}}\right) \\ \frac{1}{\sqrt{3}} \left(1 + \frac{1}{\sqrt{3}}\right) & \frac{1}{3} & -\frac{1}{\sqrt{3}} \left(1 - \frac{1}{\sqrt{3}}\right) \end{bmatrix}$$

The final form of the coordinate transformation matrix is then  $\mathbf{R} = \underline{\mathbf{R}}_1 * \underline{\mathbf{R}}_2$ , and the matrix of the Nenno-relationship becomes:

$$\underline{\mathbf{N}} = \underline{\mathbf{R}} * \underline{\mathbf{D}}.$$

Considering symmetry matrices as well, the orientation of the  $\sigma$ -phase ( $\underline{\mathbf{M}}_\sigma$ ) originating from the measurement of the orientation of the austenite, and applying the Nenno-relationship is:

$$\underline{\mathbf{M}}_{\sigma ij} = \underline{\mathbf{S}}_{\sigma j}^{-1} \underline{\mathbf{N}} \underline{\mathbf{S}}_{\gamma i} \underline{\mathbf{M}}_\gamma$$

where  $\underline{\mathbf{S}}_{\gamma i}$  is the symmetry matrix for austenite,  $\underline{\mathbf{S}}_{\sigma j}$  is that for the  $\sigma$ -phase and  $\underline{\mathbf{M}}_\gamma$  is the orientation matrix of the austenite.

Comparing the calculated  $\sigma$ -phase orientations to the measured ones it was found that the real orientation relationship differed from the ideal one (Table 3). The longer the heat treatment, the larger the difference from the ideal orientation relationship.

Table 3. Angular difference from the Nenno-relationship after heat treatment

Time of heat treatment [s]	200	500	1000	5000
Angular difference [degree]	5.7	6.6	10.4	12.6

## 5. Summary

Orientation difference between austenite and  $\sigma$ -phase was investigated in SAF 2507 type duplex steel. The matrix form of the Nenno orientation relationship was determined, and then the calculated and measured orientation relationship was compared after different heat treatments. It was found that as the duration of the heat treatment increased, the deviation from the ideal orientation relationship increased too.

## References

- [1] BÖDÖK, K., *Az ötvözetlen, gyengén és erősen ötvözött szerkezeti acélok korrózióállósága, különös tekintettel azok hegeszthetőségére*, Corweld, Budapest, 1997.
- [2] RANDLE, V., *Microtexture Determination and Its Applications*, Bourne Press, Bournemouth, United Kingdom, 1992.
- [3] SCHWARTZ, A. J. – KUMAR, M. – ADAMS, B. L., (eds.) *Electron Backscatter Diffraction in Materials Science*, Kluwer Academic/Plenum Publishers 2000.
- [4] CHEN, T. H. – YANG, J. R., *Mat. Sci. and Eng.*, **A311** (2001), pp. 28–41.
- [5] BHADESHIA, H. K. D. H., *Geometry of Crystals*, Institute of Metals, 1987.
- [6] GUNN, R. N., *Duplex Stainless Steels*, Abington Publishing, Cambridge, United Kingdom, 1997., 204 p.
- [7] SCHUMANN, H., *Kristálygeometria és a fémek rácstranzformációi*, Műszaki Könyvkiadó, Budapest, 1985.
- [8] HERBSLEB, G. – SCHWAAB, P., Precipitation of Intermetallic Compounds, Nitrides and Carbides in AF 22 Duplex Stainless Steel and their Influence on Corrosion Behavior in Acids, in: R.A. Lula, Ed., *Duplex Stainless Steels*, ASM, Metals Park, Ohio (1983), 15.
- [9] KIM, S. B. – PAIK, K. W. – KIM, Y. G., Effect of Mo Substitution by W on High Temperature Embrittlement Characteristics in Duplex Stainless Steels, *Materials Science and Engineering*, **A247** (1998), pp. 67–74.
- [10] DOBRANSZKY, J. – SZABÓ, P. J. – BEREZCZ, T. – HROTKO, V. – PORTKO, M., Energy-Dispersive Spectroscopy and Electron Backscatter Diffraction Analysis of Isothermally Aged SAF 2507 Type Superduplex Stainless Steel, *Spectrochimica Acta* **B59** (2004), pp. 1781–1788.
- [11] NENNO, S. – TAGAYA, M. – NISHIYAMA, Z., *Trans. Jpn. Inst. Met.*, **3** (1962), pp. 82–94.
- [12] KURDJUMOV, G. – SACHS, Z., *Z. Phys.*, **64** (1930), pp. 325.
- [13] SATO, Y. S. – KOKAWA, H., Preferential Precipitation Site of Sigma Phase in Duplex Stainless Steel Weld Metal, *Scripta Mater.*, **40** (1999), pp. 659–663.
- [14] LEE, K. M. – CHO, H. S. – CHOI, D. C., Effect of Isothermal Treatment of SAF 2205 Duplex Stainless Steel on Migration of  $\delta/\gamma$  Interface Boundary and Growth of Austenite, *Journal of Alloys and Compounds*, **285** (1999), pp. 156–161.